

Article

Not peer-reviewed version

---

# On the Interpretation of Cosmic Acceleration

---

[Enrique Gaztanaga](#)\*

Posted Date: 9 September 2024

doi: 10.20944/preprints202309.0873.v8

Keywords: cosmology; dark energy; general relativity; black holes



Preprints.org is a free multidiscipline platform providing preprint service that is dedicated to making early versions of research outputs permanently available and citable. Preprints posted at Preprints.org appear in Web of Science, Crossref, Google Scholar, Scilit, Europe PMC.

Copyright: This is an open access article distributed under the Creative Commons Attribution License which permits unrestricted use, distribution, and reproduction in any medium, provided the original work is properly cited.

Disclaimer/Publisher's Note: The statements, opinions, and data contained in all publications are solely those of the individual author(s) and contributor(s) and not of MDPI and/or the editor(s). MDPI and/or the editor(s) disclaim responsibility for any injury to people or property resulting from any ideas, methods, instructions, or products referred to in the content.

Article

# On the Interpretation of Cosmic Acceleration

Enrique Gaztanaga <sup>1,2,3</sup> 

<sup>1</sup> Institute of Cosmology & Gravitation, University of Portsmouth, Dennis Sciamia Building, Burnaby Road, Portsmouth PO1 3FX, UK; gaztanaga@gmail.com

<sup>2</sup> Institute of Space Sciences (ICE, CSIC), 08193 Barcelona, Spain

<sup>3</sup> Institut d'Estudis Espacials de Catalunya (IEEC), 08860 Barcelona, Spain

**Abstract:** In relativity, the Newtonian concepts of velocity and acceleration are observer-dependent quantities that vary with the chosen frame of reference. It is well established that in the comoving frame, cosmic expansion is currently accelerating; however, in the rest frame, this expansion is actually decelerating. In this paper, we explore the implications of this distinction. The traditional measure of cosmic acceleration, denoted by  $q$ , is derived from the comoving frame and describes the acceleration of the scale factor  $a$  for a 3D space-like homogeneous sphere. We introduce a new parameter  $q_E$  representing the acceleration experienced between observers within the light cone. By comparing  $q_E$  to the traditional  $q$  using observational data from Type Ia supernovae (SN) and the radial clustering of galaxies and quasars (BAO)—including the latest results from DESI2024—our analysis demonstrates that  $q_E$  aligns more closely with these data. The core argument of the paper is that  $\Lambda$ —regardless of its origin—creates an event horizon that divides the manifold into two causally disconnected regions analogous to conditions inside a black hole's interior, thereby allowing for a rest-frame perspective  $q_E$  in which cosmic expansion appears to be decelerating and the horizon acts like a friction term. Such a horizon suggests that the universe cannot maintain homogeneity outside. The observed cosmological constant  $\Lambda$  can then be interpreted not as a driver of new dark energy or a modification of gravity but as a boundary term exerting an attractive force, akin to a rubber band, resisting further expansion and preventing event horizon crossings. This interpretation calls for a reconsideration of current cosmological models and the assumptions underlying them.

**Keywords:** cosmology; dark energy; general relativity; black holes

## 1. Introduction

For over thirty years, cosmologists have accumulated compelling evidence that cosmic expansion is accelerating. More specifically, this acceleration appears to be dominated by a cosmological constant term, commonly denoted as  $\Lambda$ .

This  $\Lambda$  term can be understood in three distinct ways: (1) as a fundamental (or effective) modification of Einstein's classical general relativity (GR), denoted  $\Lambda_F$ , (2) as an effective source term from a dark energy (DE) component,  $\Lambda_{DE}$ , or (3) as a boundary term,  $\Lambda_B$ . These three possible origins can be illustrated by writing the Einstein–Hilbert action for classical GR with the corresponding additional terms:

$$S = \int_{V_4} dV_4 \left[ \frac{R}{16\pi G} + \mathcal{L}_m - \frac{\Lambda_F}{8\pi G} + \mathcal{L}_{DE} \right] + \frac{1}{8\pi G} \oint_{\partial V_4} dV_3 K. \quad (1)$$

The first two terms in the first integral represents the classical GR Lagrangian with matter-energy content  $\mathcal{L}_m$  as source term [1]. The third term corresponds to the fundamental cosmological constant  $\Lambda_F$  [2]. The fourth term is the DE or quintessence source term, given by  $\mathcal{L}_{DE} = \frac{1}{2} \bar{\nabla}^2 \psi - V(\psi)$ , for a single effective scalar field  $\psi$ . For a homogeneous perfect fluid with density  $\rho_{DE}$  and pressure  $p_{DE}$  in its ground state (where  $V \gg \dot{\psi}^2$ ), this reduces to  $\mathcal{L}_{DE} = p_{DE} = -\rho_{DE} = -\Lambda_{DE}/8\pi G$  (see also Equations (B66)–(B68) in [3]). This illustrates how  $\Lambda_F$  and  $\Lambda_{DE}$  provide totally degenerate interpretations for  $\Lambda$ .

The last integral represents the Gibbons–Hawking–York (GHY) boundary term [4–6], where  $K$  is the trace of the extrinsic curvature at the boundary  $\partial V_4 = V_3$ . As shown in [7], for a finite Friedman–Lemaître–Robertson–Walker (FLRW) metric with total mass–energy  $M_T$ , this term results in:

$$S_{GHY} = \frac{1}{8\pi G} \oint_{\partial V_4} dV_3 K = \int_{V_4} dV_4 \left[ \frac{-2\Lambda_B}{16\pi G} \right], \quad (2)$$

where  $\Lambda_B = \frac{3}{r_S^5}$ , with  $r_S = 2GM_T$ . This provides a fundamentally different origin for  $\Lambda$  compared to  $\Lambda_F$  or  $\Lambda_{DE}$ . As noted in [8], the  $\Lambda_B$  boundary term cancels the potential contributions of both  $\Lambda_F$  and  $\Lambda_{DE}$ , solving the fine tuning and coincidence problems [9].

Regardless of its origin, the  $\Lambda$  term is typically interpreted as a repulsive force between galaxies that counteracts gravity, driving the accelerated expansion of the universe. This phenomenon is often cited as one of the most profound challenges in contemporary physics and may offer a crucial observational pathway to understanding quantum gravity (e.g., see [10] and references therein).

Cosmic acceleration is typically measured using the adimensional coefficient  $q$ , defined as  $(\ddot{a}/a)H^{-2}$ , where  $H \equiv \dot{a}/a$ . If the universe follows an equation of state with  $p = \omega\rho$ , this leads to  $q = -\frac{1}{2}(1 + 3\omega)$ . For regular matter or radiation, where  $\omega > 0$ , we would expect deceleration in the expansion ( $q < 0$ ) due to gravity. However, measurements from various sources such as galaxy clustering, Type Ia supernovae, and CMB consistently show an expansion that is asymptotically approaching  $q \simeq 1$  or  $\omega \simeq -1$  (e.g., see [11] and references therein for a review of more recent results, including weak gravitational lensing). This aligns well with a cosmological constant  $\Lambda$ , where  $H^2$  approaches  $H^2 = \Lambda/3 \equiv r_\Lambda^{-2}$  and  $q$  approaches 1. What does this mean?

The term dark energy (DE) was introduced by [12] to refer to any component with  $\omega < -1/3$ . However, there is no fundamental understanding of what DE is or why we measure a term with  $\omega \simeq -1$ . A natural candidate for DE is  $\Lambda$ , which is equivalent to  $\omega = -1$  and can also be thought of as the ground state of a field (the DE), similar to the inflation but with a much smaller ( $\simeq 10^{-50} - 10^{-100}$ ) energy scale.  $\Lambda$  can also be a fundamental constant in GR, but this has some other complications ([13–15]).

This paper critically examines the conventional concept of cosmic acceleration and proposes an alternative framework for understanding cosmic expansion dynamics. In Section 2, we establish the notation and derive standard definitions for cosmic expansion in the comoving frame. In Section 3, we demonstrate the dependence of these standard definitions on the observer's frame, highlighting the lack of covariance and potential for misinterpretation in the commonly used concept of cosmic acceleration. Sections 4 and 5 introduce an alternative definition for cosmic acceleration, which is grounded in the  $\Lambda$  event horizon. In Section 6, we compare both definitions to observational data, demonstrating that our proposed approach offers greater consistency with empirical observations.

Appendix 8 provides a detailed exposition of the correct method for defining 4D acceleration in relativity based on the geodesic deviation equation. We also elaborate on the idea that  $\Lambda$  corresponds to a friction (attractive) force that decelerates cosmic events and revisit the Newtonian limit to show that  $\Lambda$  corresponds to an additional (attractive) Hooke's term to the inverse square gravitational law, envisioning a "rubber band Universe".

Finally, we conclude with a summary and discussion, emphasizing the significance of our findings for cosmological theory and observational practice and suggesting avenues for further research and exploration in the field.

## 2. Cosmic Acceleration

Current observations of the cosmos seem consistent with general relativity (GR) with a flat FLRW (Friedmann–Lemaître–Robertson–Walker) metric in comoving coordinates, corresponding to a homogeneous and isotropic space:

$$ds^2 = -d\tau^2 + a(\tau)^2 [d\chi^2 + \chi^2 d\Omega^2], \quad (3)$$

where we use units of  $c = 1$ , and  $a(\tau)$  is the scale factor. For a classical perfect fluid with matter and radiation density  $\rho = \rho_m + \rho_R$ , the solution to Einstein's field equations (called LCDM) is well known:

$$H^2 = \frac{8\pi G}{3}\rho + \frac{\Lambda}{3} \equiv H_0^2 [\Omega_m a^{-3} + \Omega_R a^{-4} + \Omega_\Lambda], \quad (4)$$

where  $\Omega_X \equiv \frac{\rho_X}{\rho_c}$ , where  $\Omega_m$  and  $\Omega_R$  represents the current ( $a = 1$ ) matter and radiation density, respectively,  $\rho_c \equiv \frac{3H_0^2}{8\pi G}$ , and  $\Omega_m + \Omega_R + \Omega_\Lambda = 1$ . The cosmological constant ( $\Lambda$ ) term corresponds to  $\Omega_\Lambda = H_0^{-2}\Lambda/3 \simeq 0.7$ , where  $H_0 \simeq 70\text{Km/s/Mpc}$ . Given  $\Omega_m \simeq 0.3$  and  $\Omega_R \simeq 4 \times 10^{-5}$ , we can use the above equations to find  $a(\tau)$  numerically.

Cosmic acceleration is usually defined as  $\ddot{a}/a$ , where the dot represents a derivative with respect to the proper time  $\tau$  at emission. A derivative over Equation (4) shows that:

$$q(z) \equiv \frac{\ddot{a}}{a} \frac{1}{H^2} = \left( \Omega_\Lambda - \frac{1}{2}\Omega_m a^{-3} - \Omega_R a^{-4} \right) \frac{H_0^2}{H^2}. \quad (5)$$

For  $\Lambda = 0$ , Equations (4) and (5) indicate that as time passes ( $a \Rightarrow \infty$ ), we have that  $H \Rightarrow 0$  and  $q \Rightarrow -1/2$ . This is because gravity opposes cosmic expansion and brings the expansion asymptotically to a halt. Including  $\Lambda$  causes the expansion to accelerate so that  $H \Rightarrow r_\Lambda^{-1}$  and  $q \Rightarrow 1$ . This is illustrated as black continuous and dashed lines in Figure 1 for  $\Omega_\Lambda = 0.7$ . The effect of  $\Lambda$  is then interpreted as a mysterious new repulsive force (or dark energy) that opposes gravity.

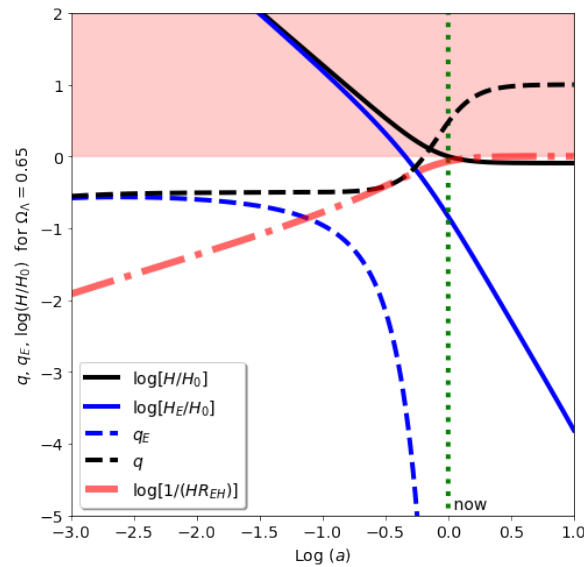


**Figure 1.** Log of cosmic expansion rate (continuous lines) and acceleration (dashed lines) as a function of time (log scale factor  $a$ ) for  $\Omega_\Lambda = 0.7$ . The black lines correspond to the usual interpretation in terms of 3D spatial coordinates:  $H$  and  $q$ . The blue lines show the corresponding results for the measurement in terms of 4D events:  $H_E$  and  $q_E$ . Without  $\Lambda$ , both are equivalent. Gravity decelerates the expansion until it asymptotically brings it to a halt ( $H \simeq H_E = 0$ ,  $q \simeq q_E = -1/2$  with an EH:  $R_{EH} \simeq \infty$ ). The effect of  $\Lambda$  according to the coordinate interpretation is to accelerate the expansion. While according to the proper distance  $R$ , it decelerates the expansion even further and brings it to an early halt:  $H_E = 0$  and  $q_E = -\infty$  at a finite horizon  $R_{EH} = r_\Lambda$ . This additional deceleration is caused by the friction term:  $1/(HR_{EH})$  in Equations (15) and (16) (dashed-dotted red line).

### 3. De Sitter Phase

The FLRW metric with  $\Lambda$  asymptotically tends to a constant:  $H = H_\Lambda$ , which corresponds to exponential inflation and de Sitter metric, which can also be written as:

$$ds^2 = -\left(1 - r^2/r_\Lambda^2\right)dt^2 + \frac{dr^2}{1 - r^2/r_\Lambda^2} + r^2d\Omega^2 \quad (6)$$

This form corresponds to a static 4D hypersphere of radius  $r_\Lambda$ . In this rest frame, events can only travel a finite distance  $r \equiv a\chi < r_\Lambda \equiv 1/H_\Lambda$  within a static 3D surface of the imaginary 4D hypersphere.

This implies that there exists a frame duality, allowing us to equivalently describe the de Sitter space either as static in proper or physical coordinates  $(t, r)$  or as exponentially expanding in comoving coordinates  $(\tau, \chi)$ . In the static frame  $(t, r)$ , events are constrained within a limited region of the hypersphere, while in the expanding frame  $(\tau, \chi)$ , distances and coordinates evolve with time following an exponential expansion characterized by the de Sitter horizon  $r_\Lambda$ .

This frame duality can be understood as a Lorentz boost that results in both length contraction and time dilation. If we define the coordinate  $r = a\chi$ , the radial velocity gives us the Hubble law  $\dot{r} = Hr$ , leading to a Lorentz factor given by

$$\gamma = \frac{1}{\sqrt{1 - \dot{r}^2}} = \left(1 - \frac{r^2}{r_H^2}\right)^{-1/2}. \quad (7)$$

where  $r_H = 1/H$ . In the rest frame  $(t, r)$ , an observer sees the moving fluid element  $ad\chi$  contracted by the Lorentz factor  $1/\gamma$  in the radial direction and experiences a time dilation by  $\gamma$ : i.e.,  $dr = ad\chi/\gamma$  and  $dt = \gamma d\tau$ . More formally, we need to find a change of variables from comoving coordinates  $(\tau, \chi)$  in the FLRW metric of Equation (3) to rest-frame de Sitter coordinates  $(t, r)$ , where  $r = a(\tau)\chi$  (see [16]):

$$-d\tau^2 + a^2d\chi^2 + a^2\chi^2d\Omega^2 = -(1 + 2\Psi)dt^2 + \frac{dr^2}{1 - r^2H^2} + r^2d\Omega^2, \quad (8)$$

which agrees with Equation (7) in [17], with:

$$(1 + 2\Psi) = \frac{a^2\dot{a}^2}{1 - r^2H^2} \left(\frac{d\tau}{d\sigma}\right)^2, \quad (9)$$

where  $\sigma = \int_0^t \chi d\chi + \int_0^\tau \frac{dt}{a(t)\dot{a}(t)}$ . This form reproduces the static de Sitter metric Equation (6) when  $H = H_\Lambda$ . It also shows that  $t$  retains its time-like character as we cross inside  $r = r_H = 1/H$ . This is to be contrasted with the event horizon of the Schwarzschild metric, which requires a change of variables as we cross inside the horizon.

The spatial part of the light element in Equation (8) is illustrated in Figure 2. Geometrically, it corresponds to the metric of a hypersphere of radius  $r_H$  that expands towards a constant radius  $r_H \Rightarrow r_\Lambda$ , which corresponds to an event horizon (see also Section 5 below and Appendix B in [16]). In the above rest (de Sitter) frame, the FLRW background is asymptotically static, indicating no expansion or acceleration, while in the comoving frame, there is cosmic acceleration ( $q = 1$ ). This observation highlights that the concept of cosmic acceleration commonly used in cosmology critically depends on the chosen frame of reference.

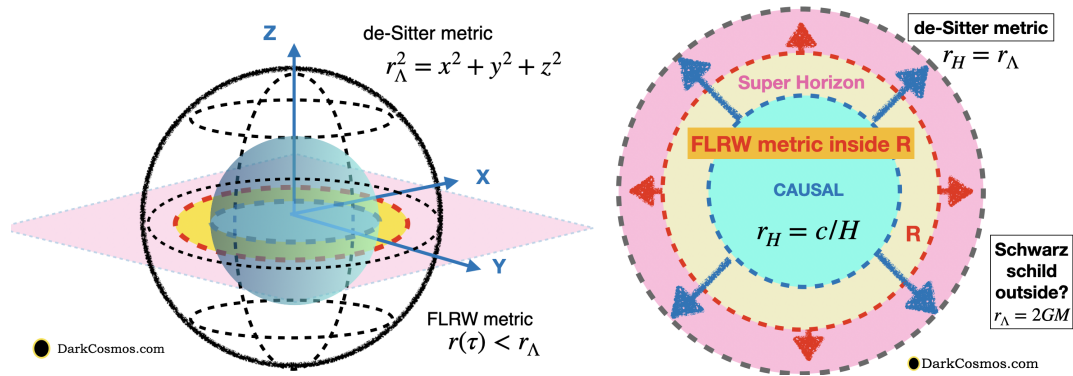


**Figure 2.** The left panel shows a spatial representation of the FLRW metric  $ds^2 = (1 - r^2/r_H^2)^{-1}dr^2 + r^2d\theta^2$  in Equation (8) as a 2D metric  $r^2 = x^2 + y^2$  (magenta plane with  $x$  and  $y$  blue arrows representing the cartesian coordinates) in polar coordinates (one angle is fixed) embedded in 3D flat space (where  $z$  in the plot corresponds to an extra dimension to illustrate the geometry). The de Sitter metric corresponds to the outer sphere  $r_H = r_\Lambda$ , while the FLRW metric is the blue sphere of radius  $r_H$  that is asymptotically expanding into  $r_\Lambda$ . The right panel shows the same 2D  $(x, y)$  plane face on, where we have also included (in red) the FLRW event horizon  $R$ , as discussed in Section 5. The yellow/blue region shows the super/sub-horizon causal regions (the arrows indicate how these regions are expanding). Scales  $r > R$  (in pink) can't be reached from inside. Because  $r > r_\Lambda$  is also causally disconnected, it has Schwarzschild metric with  $r_s = r_\Lambda = 2GM$ , when assumed empty.

#### 4. Event Acceleration

The interpretation of cosmic acceleration in Equation (5) is solely based on the definition for acceleration  $\ddot{a}/a$  in Equation (5). We next show that such a definition corresponds to events without a cause-and-effect connection, and this lead us to the wrong picture of what is happening. We will then introduce a more physical alternative.

Consider the distance between two events corresponding to the light emission of a galaxy at  $(\tau, \chi)$  and the reception somewhere in its future  $(\tau_1, \chi_1)$ . The photon travels following an outgoing radial null geodesic  $ds = 0$ , which, from Equation (3), implies  $d\tau = a(\tau)d\chi$ . This situation is depicted in Figure 3. We can define a 3D space-like distance  $d$  based in the comoving separation  $\Delta\chi = \chi - \chi_1$ :

$$d = a(\tau)\Delta\chi. \quad (10)$$

This is, in fact, the distance that corresponds to the acceleration given by  $\ddot{a}/a$  in Equation (5) because  $\dot{d}/d = \dot{a}/a$  and  $\ddot{d}/d = \ddot{a}/a$ , where the derivative is with respect to  $\tau$ , the time at emission. Such a distance corresponds to the distance between  $(\tau, \chi)$  and  $(\tau, \chi_1)$  so that  $d\tau = 0$ . These events lack causal connection and are beyond observation. While using  $d$  is not inherently incorrect, it involves extrapolating observed events (like luminosity distance) into non-observable realms. Essentially,  $d$  aligns with a non-local theory of gravity or the Newtonian approximation, where action at a distance occurs with an infinite speed of light.

We can instead use the the distance traveled by the photon:

$$d_{LC} = \int_{\tau}^{\tau_1} a(\tau)d\chi = \int_{\tau}^{\tau_1} d\tau = \Delta\tau = (\tau_1 - \tau) \quad (11)$$

Note that we use units of  $c = 1$ , so this should be read as  $d_{LC} = c\Delta\tau$ . But cosmic acceleration is zero  $\ddot{d}_{LC} = 0$  for such a distance because  $\dot{d}_{LC} = -1$ .

So the usual definition currently used by cosmologists in Equation (10) corresponds to events that are space-like, i.e., at a fixed comoving separation or fixed cosmic time  $d\tau = 0$ . It only takes into account the change in the distance due to the expansion of the universe. To have a measurement of cosmic acceleration that is closer to actual observations, we need to use the distance between events

that are causally connected, i.e., that not only takes into account how much the universe has expanded but also how long it has taken for the two events to be causally connected.

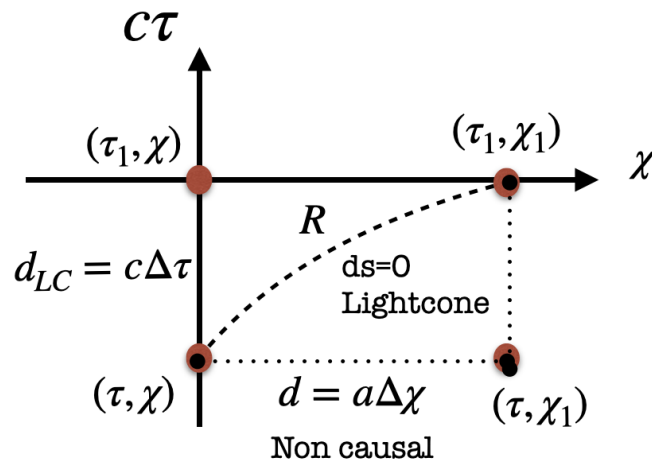


**Figure 3.** Comparison of different distances in the FLRW metric of Equation (3) between an observed event (at emission) at coordinates  $(\tau, \chi)$  and the corresponding null event (at reception) somewhere in its future  $(\tau_1, \chi_1)$ . The space-like distance  $d = a(\tau)\Delta\chi$  in Equation (10) along the horizontal  $\chi$  axis is the one commonly used to define cosmic acceleration. It expands as  $a(\tau)$ , but it is not causally connected. The distance  $d_{LC} = c\Delta\tau$  in Equation (11) along the vertical  $\tau$  axis is the time-like distance traveled by light, but it is independent of cosmic expansion  $a(\tau)$ . The event distance  $R$  in Equation (12) corresponds to the proper distance in the light-cone between the two events and is the one we should use to properly interpret cosmic expansion.

To this end, we should use the proper future light-cone distance  $R(\tau)$  obtained from  $ds = 0$  in the FLRW of Equation (3) as  $ds = 0 \Rightarrow d\chi = \int d\tau/a(\tau)$  and  $R = ad_\chi$  (see, e.g., Equation (A1) in [18]):

$$R(\tau, \tau_1) = a(\tau) \int_{\tau}^{\tau_1} d\chi = a(\tau) \int_{\tau}^{\tau_1} \frac{d\tau'}{a(\tau')} \quad (12)$$

Note that the term with the integral is not  $\Delta\chi$ , but it corresponds to the coordinate distance  $d_\chi$  traveled by light between the two events, including the effect of cosmic expansion. Thus, we argue that we should use  $R$  instead of  $d$  in Equation (10) as a measure of the distance in cosmology to define the cosmic acceleration and expansion rate. The differences between these three distances are illustrated in Figure 3.

Using  $R$  as a distance is equivalent to a simple change of coordinates in the FLRW metric of Equation (3) from comoving coordinates  $d\chi$  to physical coordinates  $dR = ad\chi$ :

$$ds^2 = -d\tau^2 + dR^2 + R^2(\tau) d\Omega^2, \quad (13)$$

which is just Minkowski's metric in spherical coordinates with a radius  $R = R(\tau)$ .

We then have that  $\dot{R} = HR - 1$ , and we define the expansion rate between null events as:

$$H_E(\tau) \equiv \frac{\dot{R}}{R} = H \left( 1 - \frac{1}{HR} \right) \quad (14)$$

where the additional term  $\frac{1}{HR}$  corresponds to a friction term. There is ambiguity in this definition because  $R$  in Equation (12) depends also on the time  $\tau_1$  used to define  $R$ . To break this ambiguity, we arbitrarily fix  $R$  to be the distance to  $\tau_1 \Rightarrow \infty$  (which corresponds to a possible future event horizon):

$$H_E(\tau) = H \left( 1 - \frac{1}{HR_{EH}} \right) \quad (15)$$

where  $R_{EH} \equiv R[\tau, \tau_1 = \infty]$ . The quantity  $\frac{1}{HR_{EH}}$  corresponds to a friction term because it opposes the expansion  $H$  that generates the term. It just originates from the change of frame. As we will see in the next section, this choice implies that  $\frac{1}{HR_{EH}}$  is zero unless  $\Lambda \neq 0$ . So this new invariant way to define cosmic expansion reproduces the standard definition when  $\Lambda = 0$ . But for  $\Lambda > 0$ , we have that the event expansion halts  $H_E \Rightarrow 0$  (blue line in Figure 1) due to the friction term (red line) for  $a \gg 1$ , while the standard Hubble rate definition approaches a constant  $H \Rightarrow \sqrt{\Lambda/3} \equiv r_\Lambda^{-1}$  (black line). This might seem irrelevant at first look, but the resulting physical interpretation is quite different. In the standard definition of  $H$ , the expansion with  $\Lambda$  becomes asymptotically exponential (or inflationary expansion), while in our new definition of  $H_E$ , the expansion becomes static (as in the static de Sitter metric).

The event acceleration can then be measured as:

$$q_E \equiv \frac{\ddot{R}}{R} \frac{1}{H_E^2} = \left( q - \frac{1}{HR_{EH}} \right) \left[ 1 - \frac{1}{HR_{EH}} \right]^{-2}. \quad (16)$$

The correct way to define 4D acceleration in relativity is based on the geodesic deviation equation: Equation (23). The relation to  $q$  and  $q_E$  will be discussed in Appendix 8.

As before, for  $\Lambda = 0$ , the friction term  $\frac{1}{HR_{EH}}$  makes little difference between  $q$  and  $q_E$ . For  $\Lambda > 0$ , the friction term asymptotically cancels the  $\Lambda$  term in  $\frac{\ddot{a}}{a}$  (i.e., Equation (5)) so that  $\frac{\ddot{R}}{R}$  is always negative, no matter how large  $\Lambda$  is ( $HR_{EH} \Rightarrow 1$  and  $q_E = -\infty$ ). The net effect of the  $\Lambda$  term is to bring the expansion of events to a faster stop ( $H_E \Rightarrow 0$ ) than in the case with gravity alone. This is illustrated in Figure 1. The  $\Lambda$  term produces a faster deceleration (than with gravity alone). This corresponds to an attracting (and not repulsive) force, as explained in more detail in Appendix 8.

## 5. Event Horizon

What is more relevant to understand the meaning of  $\Lambda$  is that the additional deceleration brings the expansion to a halt within a finite proper distance between the events, creating an event horizon (EH). The EH is the maximum distance that a photon emitted at time  $\tau$  can travel following the outgoing radial null geodesic:

$$R_{EH}(a) = a \int_a^\infty \frac{da'}{H(a')a'^2} < \frac{1}{H[a = \infty]} = r_\Lambda \equiv \sqrt{3/\Lambda} \quad (17)$$

This is illustrated in Figure 4, which also demonstrates how inflation and the horizon problem (i.e., the observation that CMB measurements detect super-horizon  $r > r_H$  frozen perturbations) occurred within  $R_{EH}$ . All the observable Universe (green line) is contained inside  $R_{EH}$ , and we can therefore not measure anything outside. In particular, we can not measure any inhomogeneities or anisotropies outside  $R$  from the inside, even if the density is discontinuous at  $R$  [16].

For  $\Lambda = 0$ , we have  $R_{EH} = \infty$ , so there is no EH. But for  $\Lambda > 0$ , we have that  $R_{EH} \Rightarrow r_\Lambda$  (red line in Figure 1). We can then see that  $\Lambda$  corresponds to a causal horizon or boundary term. The analog force behaves like a rubber band between observed galaxies (null events) that prevents them from crossing some maximum stretch (i.e., the EH). We can interpret such a force as a boundary term that just emerges from the finite speed of light (see Appendix 8 and Eq.1).

The FLRW metric with  $\Lambda$  asymptotically tends to the de Sitter metric in Equation (6). This form corresponds to a static 4D hypersphere of radius  $r_\Lambda$ . So in this (rest) frame, events can only travel a

finite distance  $R < r_\Lambda$  within a static 3D surface of the imaginary 4D hypersphere. The region inside  $r < r_\Lambda$  is causally disconnected from the outside. In the context of the FLRW framework, this condition corresponds to  $a < r_\Lambda/\chi$ , where  $\chi$  is a radial (space-like) distance. This condition implies that the expansion interpretation is valid only as long as  $a < r_\Lambda/\chi$ , indicating that it does not make sense for larger values where we cannot transition from  $r < r_\Lambda$  to  $r > r_\Lambda$ . Essentially, beyond this threshold, the cosmological interpretation of expansion breaks down due to the causal disconnection imposed by the horizon defined at  $r_\Lambda$ .

As shown in Equation (8), this frame duality can be understood as a Lorentz boost. An observer in the rest frame sees the moving fluid element  $ad\chi$  contracted by the Lorentz factor  $\gamma$ . This duality is better understood using our new measures for the expansion rate  $H_E$  and cosmic deceleration  $q_E$  based on the distance between causal events.

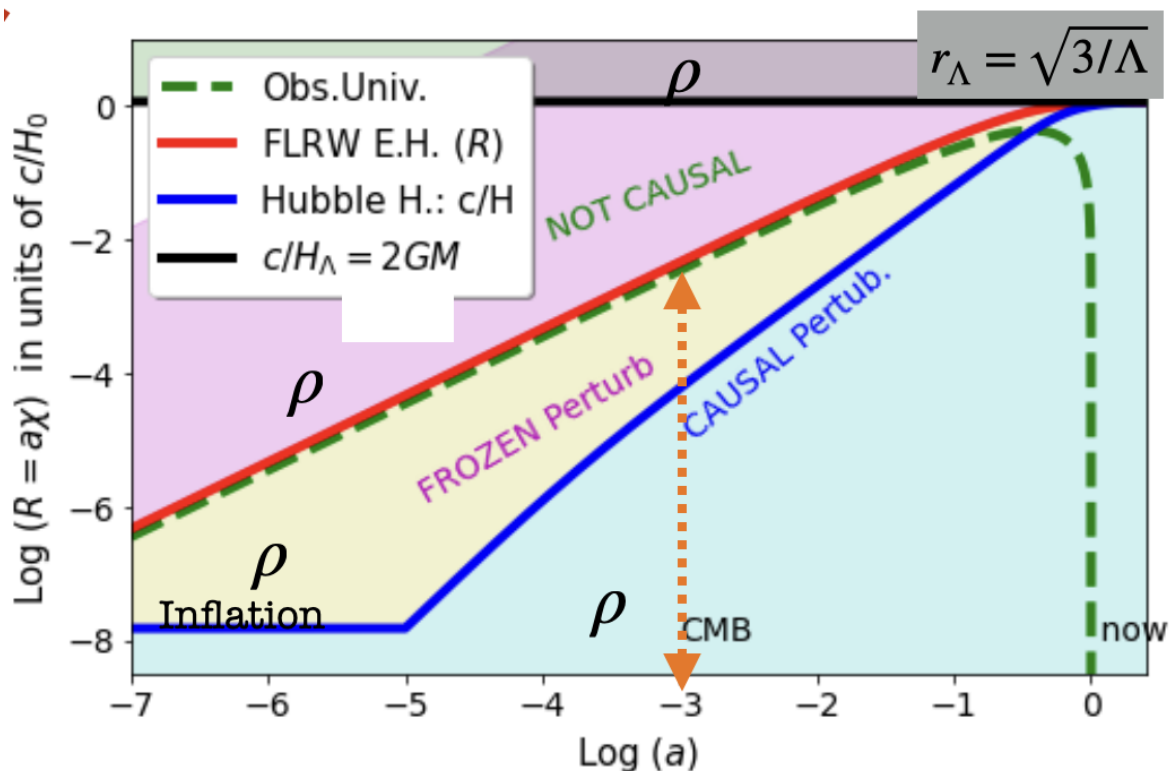


**Figure 4.** Proper coordinate  $r = a(\tau)\chi$  in units of  $c/H_0$  as a function of cosmic time  $a$  (scale factor). The Hubble horizon  $r_H = c/H$  (blue continuous line) is compared to the  $\Lambda$  future event horizon  $R_{EH}$  (red line) as defined in Equation (17). Larger radii (magenta shading) represent causally disconnected regions, while smaller ones (yellow shading), created during cosmic inflation, remain dynamically frozen. The full observable universe (dashed green line) encompasses both causal (blue shading) and frozen regions. Note how the observable region is bounded by  $r < R_{EH}$ : we can not measure any inhomogeneities or anisotropies even if the density is discontinuous at  $R$ . Compare to Figure 2, which depicts a view at a fixed  $a$  using the same color coding. After inflation,  $r_H$  begins growing again, and by  $a \approx 1$  (present epoch), both  $r_H$  and  $R_{EH}$  approach  $r_\Lambda$  (in black). The vertical dash orange arrows indicate the CMB epoch.

## 6. Comparison to Data

We show next how to estimate the new measure of cosmic acceleration  $q_E$  using direct astrophysical observations. As an example, consider the Supernovae Ia (SNIa) data as given by the “Pantheon Sample” compilation ([19]) consisting of 1048 SNIAs between  $0.01 < z < 2.3$ . Each SNIa provides a

direct estimate of the luminosity distance  $d_L(z)$  at a given measured redshift  $z$ . This corresponds to the comoving look-back distance:

$$\chi(z) = ad_L(z) = \int_0^z \frac{dz}{H(z)} \quad (18)$$

so that  $\chi' \equiv d\chi/dz$  directly gives us  $\chi' = r_H = H^{-1}$ . The second derivative gives us the acceleration:

$$q = 1 + \frac{\chi''}{a\chi'} ; \quad q_E = \frac{q - \chi'/R_{EH}}{(1 - \chi'/R_{EH})^2}. \quad (19)$$

$R_{EH}$  is given by the model prediction in Equation (17) (arbitrarily fixed at  $\Omega_\Lambda = 0.85$  in both data and models). We adopt here the approach presented in [20], which used an empirical fit to the luminosity distance measurements based on a third-order logarithmic polynomial:

$$\chi(a) = ad_L = a \left( x + Ax^2 + Bx^3 \right) H_0^{-1} \ln 10 \quad (20)$$

where  $x = -\log_{10} a$ . The authors of [20] find a good fit using  $A = 3.15 \pm 0.12$  and  $B = 3.27 \pm 0.41$  for the full SNIa ‘‘Pantheon Sample’’. We use these values of  $A$  and  $B$  and their corresponding errors to estimate  $H$ ,  $q$ , and  $q_E$  using the above relations. The results for  $H$  and  $q$  are shown as shaded cyan regions in the left panel of Figure 5. They are compared to the LCDM predictions (dashed lines) in Equations (4) and (5).

There is very good agreement in  $H(z)$  for  $\Omega_\Lambda \simeq 0.65$ . At  $z < 1$ , the  $q(z)$  estimates are also consistent with the  $\Omega_\Lambda \simeq 0.65$  predictions. But the detailed  $q(z)$  evolution with redshift in the SNIa data does not seem to follow any of the model predictions, especially for  $z > 1$ . The  $q(z)$  estimates are too steep compared to the different models’ predictions. If we compare instead the  $q_E$  estimates (see right panel of Figure 5), we find much better agreement with the model predictions. This seems to validate our  $q_E$  approach, but it is not clear from this comparison alone if this is caused by the fitting function used in Equation (20).

To test this further, we use measurements of the radial BAO data to estimate  $q_E$ . Such measurements give us a direct estimate of  $H(z)$  (as first demonstrated by [21]), so they have the advantage over SNIa in that we only need to do a first-order derivative to estimate  $q$  or  $q_E$ :

$$q = 1 + \frac{1}{aH} \frac{dH}{dz} ; \quad q_E = \frac{q - r_H/R_{EH}}{(1 - r_H/R_{EH})^2}. \quad (21)$$

As an illustration, we utilize the  $H(z)$  measurements presented in Table 2 of [22], which provide an expanded dataset that includes results up to 2023. This compilation of  $H(z)$  values is shown as red points with  $2\sigma$  error bars in the left panel of Figure 5 and is labeled as ‘‘<2023’’. Additionally, we incorporate four new data points from DESI2024 (LRG1, LRG2, LRG3+ELG1, and ELG2) derived from Table 18 of [23], using a sound horizon  $r_o = 147$  Mpc from CMB measurements [24] to obtain  $H(z)$ , along with one data point from the Ly-alpha forest as described in Equation (7.3) of [25]. These are displayed as blue points with  $2\sigma$  error bars in the left panel of Figure 5 and are labeled as ‘‘DESI2024’’.

The full compilation includes measurements from galaxy clustering ( $z < 1.5$ ) and the Ly-alpha forest in quasars ( $z > 2$ ). The combination of these distinct redshift ranges provides a robust measurement of  $\frac{dH}{dz}$  at intermediate redshifts ( $1 < z < 2$ ), where discrepancies in the supernova Type Ia data are observed when comparing the traditional  $q$  model and the  $q_E$  model (as discussed earlier). The radial BAO offers strong constraints on cosmic acceleration that are independent of potential calibration errors in  $H_0$  or sampling biases from small-area surveys. This level of precision is something that is not yet achievable with current supernova datasets, but it will be exciting to see how upcoming wider and deeper surveys might address this issue in the near future.

We fit a quadratic polynomial with inverse variance weighting to the radial BAO data:

$$H(z) = H_0 + H_1 z + H_2 z^2. \quad (22)$$

In units of Km/s/Mpc, we find  $H_0 \simeq 69 \pm 3$ ,  $H_1 \simeq 37 \pm 6$  and  $H_2 \simeq 14 \pm 2$ , with strong covariance between the errors (the cross-correlation coefficient between  $H_1$  and  $H_2$  is  $-0.965$ ). The value of  $H_0$  is in good agreement with the Planck CMB fit [24] but is in some tension with the SNIa local calibration:  $H_0 = 73 \pm 1$  (see [26]). This corresponds to either a local calibration problem (in SNIa, in radial BAO, or in both) or tension in the  $\Lambda$ CDM model at different times or distances (see, e.g., [27]). We ignore this normalization problem here and just focus on the evolution of  $H/H_0$  to measure cosmic acceleration  $q$  or  $q_E$  (which are fairly independent of  $H_0$ ).

In the right panel of Figure 5, we show (as shaded regions) the measurements for  $q_E$  given by combining Equation (20) with Equation (19) and Equation (22) with Equation (21). The measurements clearly favor models with large negative cosmic event acceleration  $q_E < 0$ , which supports our interpretation of  $\Lambda$  as a friction term.

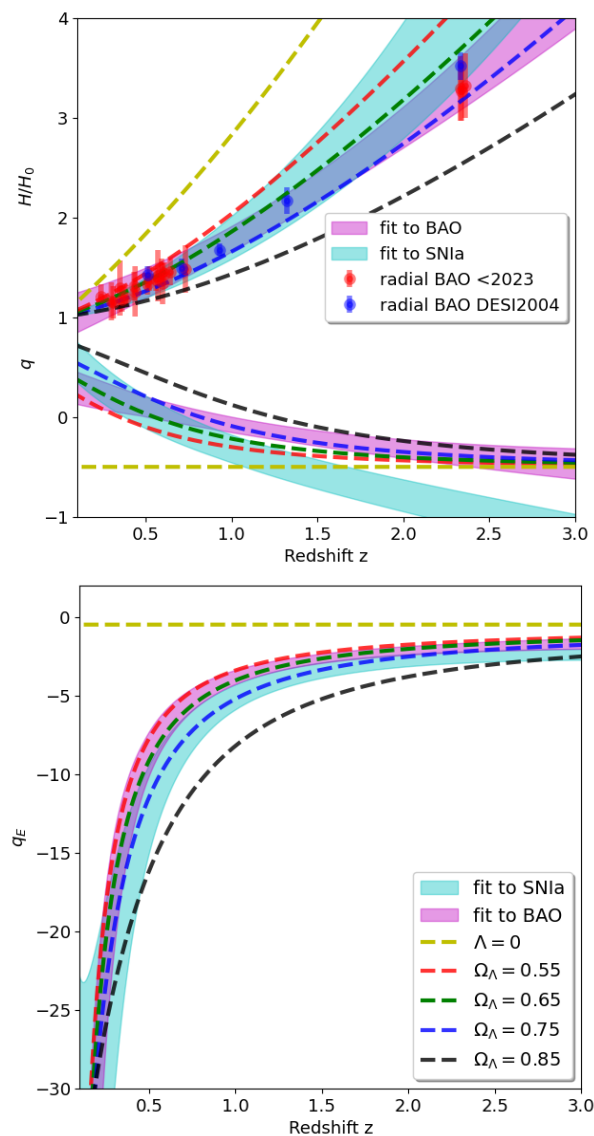


**Figure 5.** Expansion rate  $H(z)$  (upper left panel), cosmic acceleration  $q$  (lower left panel), and event acceleration  $q_E$  (right panel). Shaded areas correspond to a polynomial fit with a  $2\sigma$  region in a sample of SNIa (cyan) and radial BAO measurements (magenta). Dashed lines show the corresponding LCDM predictions for different values of  $\Omega_\Lambda$  as labeled.

Comparing the left and right panels in Figure 5, we see that both  $q$  and  $q_E$  are roughly consistent with models with  $\Omega_\Lambda \simeq 0.7$  (or  $\Lambda \simeq 2H_0^2$ ), in good concordance with  $H(z)$  in the upper left panel of Figure 5.

Even when the underlying model for  $q$  and  $q_E$  is the same, note how the measured  $q$  and  $q_E$  data have different tensions with the model predictions as a function of redshift. In particular, the radial BAO and SNIa datasets show inconsistencies among them for  $q$  around  $1.5 < z < 3.0$ . This is a known tension (see, e.g., Figure 17 in [28]). But note how this tension disappears when we use the corresponding estimates for  $q_E$ . Thus, data are more consistent with the  $q_E$  than with the  $q$  description.

One would expect that a perfect realizations of the LCDM model in Equation (4) would produce consistent results in both  $q$  and  $q_E$ . But deviations from LCDM and systematic effects can produce tensions in data, especially if we use a parametrization like  $q$  that refers to events that we never observe. The  $q$  and  $q_E$  parametrizations of acceleration are more general than the particular LCDM model, and the fact that data prefer  $q_E$  is an important indication. Data live in the light-cone, which corresponds to  $q_E$  rather than  $q$ . At  $z \simeq 2$ , the difference between a light-cone and space-like separations is very significant, and any discrepancies in the data or model will be more pronounced in  $q$  modeling.

We conclude that the data show some tensions with LCDM predictions (as indicated by  $q$ ) but confirm that cosmic expansion is clearly decelerating (as indicated by  $q_E$ ) so that events are trapped inside an event horizon ( $R_{EH}$ ).

## 7. Discussion and Conclusions

In our exploration, we have demonstrated that the commonly interpreted  $\Lambda$  term, thought to drive cosmic acceleration (as discussed in Section 2), actually leads to a quicker cosmic deceleration of events compared to the influence of gravity alone (as explained in Section 4). This relates to the nature of the event horizon (EH) (see Section 5) that results from an expansion dominated by  $\Lambda$ . It suggests that  $\Lambda$  might not be a new form of dark or vacuum energy  $\Lambda_{DE}$  ([13–15]) or a modification of gravity  $\Lambda_F$  but rather a boundary or surface term  $\Lambda_B$  in the corresponding action (see Equation (1)).

The measured  $R_{EH}$  in our cosmic expansion exhibits behavior analogous to the interior of a Schwarzschild black hole (BH), particularly under the assumption of nearly empty space beyond  $R_{EH}$  (see [16]). This analogy is illustrated in Figures 2 and 4, which challenge the conventional interpretation of the FLRW metric. The FLRW model assumes that the background density  $\rho$  remains constant both inside and outside  $R_{EH}$ , despite the absence of causal connections between these regions. How could this be possible?

The absence of causality suggests that the universe could be inhomogeneous outside  $R_{EH}$  while remaining homogeneous within  $R_{EH}$ , as indicated by cosmic expansion. This concept diverges from the traditional horizon problem as described by [3,29], in which the standard cosmological model envisions a homogeneous and isotropic universe fragmented into approximately  $10^{83}$  causally disconnected regions in the past [30].

Inflationary theory, initially proposed by [31] and further developed by [30,32,33], addresses the problem of cosmological fragmentation. It posits a period of exponential expansion driven by a state of energy characterized by the ground state of a field that translates into an effective negative pressure (similar to  $\mathcal{L}_{DE} = p_{DE} = -\rho_{DE}$  in Equation (1)). This foundational phase allows scales to initially exit the Hubble horizon (as depicted in the yellow regions of Figures 2 and 4) and to re-enter post-inflation. Despite its success, the origins of this inflationary period remain elusive, posing a significant mystery in theoretical physics. Furthermore, inflationary theory does not address the causality outside  $R_{EH}$  (see Figure 4), raising critical considerations for our understanding of the Universe's expansion.

The event horizon  $R_{EH}$  measured with  $q_E$  (i.e., Equation (17), which is equivalent to the presence of  $\Lambda$ ) also tells us that there is a finite mass  $M_T$  trapped within  $R_{EH}$ . If we assume that the space outside  $R_{EH}$  is relatively empty, such a finite mass  $M_T$  provides the explanation for the observed  $R_{EH}$  and, therefore, for  $\Lambda$ : i.e.,  $2GM_T = \sqrt{3/\Lambda}$  as resulting from a boundary term (see Equation (1)). This black hole Universe (BHU) model provides a new and completely classical explanation for the

cosmological constant  $\Lambda$  within GR. It explains why  $\Lambda$  is so small but not zero: because  $M_T$  is so large but not infinite. Yet it also raises new fundamental questions: If our local universe has fallen inside its own gravitational radius  $r_s = 2GM_T = \sqrt{3/\Lambda}$ , why is our universe now expanding and not collapsing?

The BHU interpretation, where the expansion happens inside  $R_{EH}$  (and is therefore a local solution [16]), opens the way to a new conjecture for the origin of cosmic expansion. Instead of emerging from a singular Big Bang (a global solution), it could result from the cold collapse of a large and low-density (local) cloud into a black hole. Such a collapse originates from a small initial over-density within a flat background, which can be modeled as a local FLRW closed curvature  $k = 1/\chi_*^2 > 0$  solution, where the curvature radius  $\chi_*$  is the comoving radius of the initial cloud. Note that [16] focused on the junction conditions for a flat  $k = 0$  case (which is the right approximation for our expanding universe or a flat expanding perturbation). The corresponding case with curvature during collapse was solved in §12.5.1 of [34], with the only difference with respect to the  $k = 0$  being the replacement of the adimensional  $\chi$  by  $\sin(\chi)$ . The total relativistic mass  $M_T$  of the collapsing cloud is also given by  $2GM_T = r_s \simeq H_0^2 \chi_*^2$ , which relates to both  $\Lambda$  (as a boundary term:  $r_s = r_\Lambda$ ) and the initial curvature radius  $k = 1/\chi_*^2$ . As the collapse approaches the almost singular ground state, the curvature increases as  $H^2 \simeq k/a^2$ , which, together with positive background acceleration (from the degenerate ground state), enables the bounce to happen. After the bounce, the inflationary expansion erases the curvature term, while  $r_\Lambda$  will eventually dominate the bouncing expansion. This is illustrated in Figure 6, which is reproduced from [9]. Unlike traditional models that lead to a singularity, this model suggests that a Big-Bang-like explosion—termed the Big Bounce—prevents such an outcome. This Big Bounce could be driven by neutron degeneracy pressure, which occurs when densely packed neutron matter reaches a ground state governed by the Pauli exclusion principle. It could also be the result of a similar ground state happening at higher energies, like in standard cosmic inflation.

Mirroring the dynamics predicted by cosmic inflation, a ground state acts like a relativistic fluid with negative pressure in a closed cloud ( $k > 0$ ). The combination of these two ingredients (positive curvature and positive background acceleration) not only halts the gravitational collapse but also catalyzes a fast rebound (exponential expansion that erases the original curvature), initiating the expansive phase of a flat Big Bang. The expansion drives the system away from the ground state, but the system returns to regular radiation- and, later, matter-domination phases. This expansion is eventually stopped by another quasi-de Sitter phase, this time caused by the finite mass of the system  $R_{EH} \rightarrow 2GM_T = \sqrt{3/\Lambda}$ . Crucially, this quantum mechanism (Pauli exclusion principle) violates the strong energy condition  $\rho + 3p \geq 0$  (but not the weak one  $\rho + p \geq 0$ ) in classical general relativity (GR) within a closed metric ( $k > 0$ ) and sidesteps the singularity GR theorems proposed by Hawking and Penrose (e.g., [35]), thus presenting a novel solution to a pivotal issue in cosmological theory.

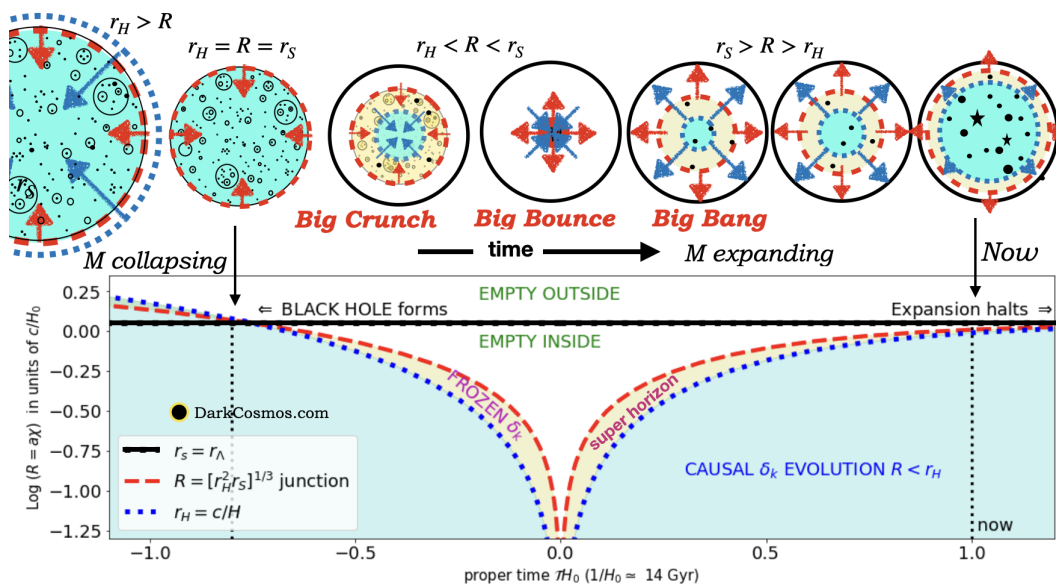


**Figure 6.** Illustration of the formation of a BHU, where  $R = R_{EH}$  is the event horizon. Colored regions  $r < R$  (dashed red line) are filled with a uniform FLRW metric (blue corresponds to  $r < r_H$  and yellow corresponds to  $r > r_H$ ) with empty space outside. A cloud of radius  $R$  and mass  $M$  collapses under gravity. When it reaches  $R = r_S = 2GM$ , it becomes a BH. The collapse proceeds inside the BH (where a frozen layer  $r > r_H$  appears in yellow) until it bounces, producing an expansion (the hot Big Bang). The event horizon  $r_S$  behaves like a cosmological constant with  $\Lambda = 3/r_S^2$  so that the expansion freezes before it reaches back to  $r_S = r_\Lambda \equiv 1/H_\Lambda$ . The bottom panels shows the evolution of  $R$  and  $r_H$  during collapse and expansion in log units of  $1/H_0$ . The structure in between  $R$  and  $r_H$  is frozen and seeds structure formation in our Universe, which could include smaller BHUs, CMB, stars, and galaxies, and replaces the role of inflation in  $\Lambda$ CDM (from [9]).

This idea is further validated by the observed large-scale cut-off in the scale-invariance spectrum of metric perturbations, as observed in the CMB sky (see [36]). Such a cut-off is measured to be 66 degrees, which corresponds to the  $R_{EH}$  radius at recombination (see dotted horizontal line in Figure 4) projected in the CMB sky. Recent research ([37]) has further revealed that several large-scale persistent CMB temperature anomalies originate from parity asymmetry  $\mathcal{P}$ . A groundbreaking explanation posits that the microscopic laws of quantum physics adhere to  $\mathcal{PT}$  symmetry in a way that preserves causality and promotes curved spacetimes. Cosmic evolution disrupts the  $\mathcal{T}$  symmetry, resulting in the observed  $\mathcal{P}$  asymmetry. This idea was originally applied to inflationary quantum fluctuations but can be equally applied to the BHU Big Bounce picture explained above, as they are both defined by a period of quasi-de Sitter expansion.

Additionally, we can conjecture from this notion that the interior dynamics of any other BH (e.g., stellar, binary, or galactic) could also result from a similar BHU solution: a classical and non-singular FLRW expanding interior (that becomes asymptotically de Sitter, i.e., static in the rest frame). The mass (equivalent to  $\Lambda$ ) boundary term in the BHU can then be interpreted as the actual physical mechanism that prevents anything from escaping the BH interior: i.e., it prevents the inside-out crossing of the BH event horizon  $r_S = 2GM = r_\Lambda$ , which asymptotically results from  $R_{EH} \rightarrow r_\Lambda$ .

That the measured  $\Lambda$  term is fixed by the total mass  $M_T$  of our universe is in good agreement with the physical interpretation presented here that  $R_{EH}$ , in the rest frame, corresponds to a friction (attractive) force that decelerates cosmic events. In Appendix 8, we elaborate on this idea and revisit the Newtonian limit to show that  $\Lambda$  corresponds to an additional (attractive) Hooke's term to the inverse square gravitational law.

**Funding:** This work was partially supported by grants from Spain MCIN/AEI/10.13039/501100011033, grants PGC2018-102021-B-100 and PID2021-128989NB-I00, from the Unidad de Excelencia María de Maeztu CEX2020-

001058-M, and from European Union funding LACEGAL 734374 and EWC 776247. IEEC is funded by Generalitat de Catalunya.

**Data Availability Statement:** No new data are presented.

**Acknowledgments:** I would like to thank K. Sravan Kumar, Benjamin Camacho-Quevedo, Pablo Fosalba, Elizabeth Gonzalez, and Pablo Renard for comments on the manuscript.

**Conflicts of Interest:** The author declare no conflicts of interest.

## 8. Newtonian and Hookeonian Limits

When we talk about classical forces, we are making an analogy to Newton's law to gain some intuition on the physical problem. This is why we study next the role of  $\Lambda$  in the non-relativistic limit. Consider the geodesic acceleration  $g^\mu = (g^0, g^i) = (g^0, \vec{g})$  defined from the geodesic deviation equation (see [34]):

$$g^\mu \equiv \frac{D^2 v^\mu}{D\tau^2} = R^\mu_{\alpha\beta\gamma} u^\alpha u^\beta v^\gamma, \quad (23)$$

where  $v^\mu$  is the separation vector between neighboring geodesics, and  $u^\alpha$  is the vector tangent to the geodesic. For an observer following the trajectory of the geodesic  $u^\alpha = (1, 0)$  and  $g^\alpha = (0, \vec{g})$ :

$$g^i = R^i_{00\gamma} v^\gamma. \quad (24)$$

and we can choose the separation vector  $v^\mu$  to be the spatial coordinate. The spatial divergence of  $\vec{g}$  is then:

$$\vec{\nabla} \cdot \vec{g} = R^0_0 = -4\pi G(\bar{\rho} + 3\bar{p}) + \Lambda = 3\frac{\ddot{a}}{a}. \quad (25)$$

This equation is always valid for a comoving observer (see Equation (6.105) in [34]). Newtonian gravity is reproduced for the case of non-relativistic matter ( $\bar{p}/c^2 \simeq 0$ ). The gravitational force (without  $\Lambda$ ) is always attractive for  $\bar{p} = 0$  (because  $\bar{\rho} > 0$ , and therefore,  $\vec{\nabla} \cdot \vec{g} < 0$ ), but it can be repulsive when  $\bar{p} < -\bar{\rho}/3$ . For example, in the case of pure vacuum energy with  $\Lambda = 0$ , we have  $p_{vac} = -\rho_{vac}$  and a repulsive gravitational force  $\vec{\nabla} \cdot \vec{g} = +8\pi G\rho_{vac}$ . The covariant version of Equation (25) is the relativistic version of Poisson's Equation (see also [8,38]):

$$\nabla_\mu g^\mu = R^0_0 = -4\pi G(\bar{\rho} + 3\bar{p}) + \Lambda = 3\frac{\ddot{a}}{a}. \quad (26)$$

The solution to these equations is given by an integral over the usual propagators or retarded Green functions, which account for causality.

This is also the Raychaudhuri equation for a shear-free, non-rotating fluid, where  $\Theta = \nabla_\nu u^\nu$ , and  $u^\nu$  is the 4-velocity:

$$\nabla_\mu g^\mu = \frac{d\Theta}{d\tau} + \frac{1}{3}\Theta^2 = R_{\mu\nu} u^\mu u^\nu = -4\pi G(\rho + 3p) + \Lambda \quad (27)$$

The above equation is purely geometric: it describes the evolution in proper time  $\tau$  of the dilatation coefficient  $\Theta$  of a bundle of nearby geodesics. Note that without  $\Lambda$ , the acceleration is always negative unless  $p < -1/3\rho$ , which is what we call DE today. This is degenerate with the  $\Lambda$  term for constant  $p = -\rho$ , so we can argue that  $\Lambda$  is a particular case of DE (but it can also be interpreted as a modified gravity term).

In the non-relativistic limit, we see from Equation (25) that, indeed,  $\ddot{a}/a > 0$  corresponds to a repulsive force that dominates at large distances. For a point-like source,

$$\vec{g}(\vec{r}) = -\frac{GM\hat{r}}{r^2} + \frac{\Lambda}{3}\vec{r} \quad (28)$$

and acceleration can only be caused by  $\Lambda$  (see also [38,39]). Note how the linear term has the wrong sign compared to Hooke's law. It actually makes little sense to take the strict non-relativistic limit in

cosmology because in that limit, photons from different times will reach us instantly, as in Equation (10). To make sense of observations, we need to take into account the intrinsically relativistic effect that the speed of propagation is finite ( $c = 1$ ). This corresponds to an additional term to the covariant acceleration  $\nabla_\mu g^\mu$ , which results in Equation (16). So besides gravitational deceleration, there is also a friction term proportional to  $H$  that is caused by the expansion itself:

$$\vec{\nabla} \vec{g} = -4\pi G(\bar{\rho} + 3\bar{p}) + \Lambda - 3\frac{H}{R_{EH}} \quad (29)$$

So the corresponding point like source is:

$$\vec{g}(\vec{r}) = -\frac{GM\hat{r}}{r^2} - \left(\frac{H}{R_{EH}} - \frac{\Lambda}{3}\right)\vec{r} \quad (30)$$

The negative friction term is always larger than the positive  $\Lambda$  term and asymptotically cancels it. This changes the sign of our interpretation of the role of  $\Lambda$  in terms of classical forces. The additional term now has the standard sign of Hooke's law in the above equation, so the effect of the  $\Lambda$  term can just be interpreted as a rubber-band-like force that prevents crossing of the EH. We can summarize this as:  $\Lambda$  accelerates the 3D coordinate spatial expansion in  $a(\tau)$ , and this causes an additional deceleration in the expansion of events, which results in an EH or a trapped surface.

## References

- Hilbert, D. Die Grundlage der Physik. *Konigl. Gesell. Wiss. Göttingen Math. Phys. K* **1915**, 3, 395–407.
- Einstein, A. Kosmologische Betrachtungen zur allgemeinen Relativitätstheorie. In *Sitzungsberichte der Königlich Preussischen Akademie der Wissenschaften (Berlin)*; 1917; pp. 142–152.
- Weinberg, S. *Cosmology*; Oxford University Press: Oxford, UK, 2008.
- York, J.W. Role of Conformal Three-Geometry in the Dynamics of Gravitation. *Phys. Rev. Lett.* **1972**, 28, 1082–1085.
- Gibbons, G.W.; Hawking, S.W. Cosmological event horizons, thermodynamics, and particle creation. *Phys. Rev. D* **1977**, 15, 2738–2751.
- Hawking, S.W.; Horowitz, G.T. The gravitational Hamiltonian, action, entropy and surface terms. *Class Quantum Gravity* **1996**, 13, 1487.
- Gaztañaga, E. The mass of our observable Universe. *Mon. Not. R. Astron. Soc.* **2023**, 521, L59–L63.
- Gaztañaga, E. The cosmological constant as a zero action boundary. *Mon. Not. R. Astron. Soc.* **2021**, 502, 436–444.
- Gaztañaga, E. The Black Hole Universe, Part II. *Symmetry* **2022**, 14, 1984. <https://doi.org/10.3390/sym14101984>.
- de Boer, J.; Dittrich, B.; Eichhorn, A.; Giddings, S.B.; Gielen, S.; Liberati, S.; Livine, E.R.; Oriti, D.; Papadodimas, K.; Pereira, A.D.; et al. Frontiers of Quantum Gravity: Shared challenges, converging directions. *arXiv* **2022**, arXiv:2207.10618.
- DES Collaboration. DES Year 3 results: Cosmological constraints from galaxy clustering and weak lensing. *Phys. Rev. D* **2022**, 105, 023520.
- Huterer, D.; Turner, M.S. Prospects for probing the dark energy via supernova distance measurements. *Phys. Rev. D* **1999**, 60, 081301.
- Weinberg, S. The cosmological constant problem. *Rev. Mod. Phys.* **1989**, 61, 1–23.
- Carroll, S.M.; Press, W.H.; Turner, E.L. The cosmological constant. *Annu. Rev. Astron. Astrophys.* **1992**, 30, 499–542.
- Peebles, P.J.; Ratra, B. The cosmological constant and dark energy. *Rev. Mod. Phys.* **2003**, 75, 559–606.
- Gaztañaga, E. The Black Hole Universe, Part I. *Symmetry* **2022**, 14, 1849. <https://doi.org/10.3390/sym14091849>.
- Lochan, K.; Rajeev, K.; Vikram, A.; Padmanabhan, T. Quantum correlators in Friedmann spacetimes: The omnipresent de Sitter spacetime and the invariant vacuum noise. *Phys. Rev. D* **2018**, 98, 105015. <https://doi.org/10.1103/PhysRevD.98.105015>.
- Ellis, G.F.R.; Rothman, T. Lost horizons. *Am. J. Phys.* **1993**, 61, 883–893.

19. Scolnic, D.M.; Jones, D.O.; Rest, A.; Pan, Y.C.; Chornock, R.; Foley, R.J.; Huber, M.E.; Kessler, R.; Narayan, G.; Riess, A.G.; et al. The Complete Light-curve Sample of Spectroscopically Confirmed SNe Ia from Pan-STARRS1 and Cosmological Constraints from the Combined Pantheon Sample. *Astrophys. J.* **2018**, *859*, 101.
20. Liu, Y.; Cao, S.; Biesiada, M.; Lian, Y.; Liu, X.; Zhang, Y. Measuring the Speed of Light with Updated Hubble Diagram of High-redshift Standard Candles. *Astrophys. J.* **2023**, *949*, 57.
21. Gaztañaga, E.; Cabré, A.; Hui, L. Clustering of luminous red galaxies - IV. Baryon acoustic peak in the line-of-sight direction and a direct measurement of  $H(z)$ . *Mon. Not. R. Astron. Soc.* **2009**, *399*, 1663–1680.
22. Niu, J.; Chen, Y.; Zhang, T.J. Reconstruction of the dark energy scalar field potential by Gaussian process. *arXiv* **2023**, arXiv:2305.04752.
23. DESI Collaboration. DESI 2024 III: Baryon Acoustic Oscillations from Galaxies and Quasars. *arXiv* **2024**, arXiv:2404.03000.
24. Planck Collaboration. Planck 2018 results. VI. Cosmological parameters. *Astron. Astrophys.* **2020**, *641*, A6.
25. DESI Collaboration. DESI 2024 IV: Baryon Acoustic Oscillations from the Lyman Alpha Forest. *arXiv* **2024**, arXiv:2404.03001.
26. Riess, A.G. The expansion of the Universe is faster than expected. *Nat. Rev. Phys.* **2019**, *2*, 10–12.
27. Abdalla, E.; et al. Cosmology intertwined: A review of the particle physics, astrophysics, and cosmology associated with the cosmological tensions and anomalies. *J. High Energy Astrophys.* **2022**, *34*, 49–211.
28. Bautista, J.; et al. Measurement of baryon acoustic oscillation correlations at  $z = 2.3$  with SDSS DR12 Ly $\alpha$ -Forests. *Astron. Astrophys.* **2017**, *603*, A12.
29. Rindler, W. Visual horizons in world models. *Mon. Not. R. Astron. Soc.* **1956**, *116*, 662.
30. Guth, A.H. Inflationary universe: A possible solution to the horizon and flatness problems. *Phys. Rev. D* **1981**, *23*, 347–356.
31. Starobinskiĭ, A.A. Spectrum of relict gravitational radiation and the early state of the universe. *Soviet J. Exp. Ther. Phys. Lett.* **1979**, *30*, 682.
32. Linde, A.D. A new inflationary universe scenario. *Phys. Lett. B* **1982**, *108*, 389–393.
33. Albrecht, A.; Steinhardt, P.J. Cosmology for Grand Unified Theories with Radiatively Induced Symmetry Breaking. *Phys. Rev. Lett.* **1982**, *48*, 1220–1223.
34. Padmanabhan, T. *Gravitation*; Cambridge University Press: Cambridge, UK, 2010.
35. Hawking, S.W.; Penrose, R.; Bondi, H. The singularities of gravitational collapse and cosmology. *Proc. R. Soc. Lond. A Math. Phys. Sci.* **1970**, *314*, 529–548.
36. Gaztañaga, E.; Camacho-Quevedo, B. What moves the heavens above? *Phys. Lett. B* **2022**, *835*, 137468. <https://doi.org/10.1016/j.physletb.2022.137468>.
37. Gaztañaga, E.; Sravan Kumar, K. Finding origins of CMB anomalies in the inflationary quantum fluctuations. *J. Cosmol. Astropart. Phys.* **2024**, *in press*. <https://doi.org/10.1088/1475-7516/2024/06/001>
38. Gaztañaga, E. The size of our causal Universe. *Mon. Not. R. Astron. Soc.* **2020**, *494*, 2766–2772.
39. Calder, L.; Lahav, O. Dark energy: Back to Newton? *Astron. Geophys.* **2008**, *49*, 1.13–1.18.

**Disclaimer/Publisher's Note:** The statements, opinions and data contained in all publications are solely those of the individual author(s) and contributor(s) and not of MDPI and/or the editor(s). MDPI and/or the editor(s) disclaim responsibility for any injury to people or property resulting from any ideas, methods, instructions or products referred to in the content.